Mimicking nature:

Physical basis and artificial synthesis of the Lotus-effect

S.C.S. Lai (0020370)
August 2003
Universiteit Leiden

Table of contents

0. Introduction

In several Asian religions the Lotus flower (*Nelumbo Nucifera*) is revered as the symbol of purity. The basis of this consideration is based on the self-cleansing property of the leaves of the Lotus flower: even when emerging from muddy waters the leaves unfold untouched by the pollution. This property of self-cleansing has been researched thoroughly and is ascribed to the interaction between the surface of the Lotus-leaves and the water, resulting in high water-repellency of the surface. Due to the impressive demonstration of these self-cleansing and high water-repellency characteristics by the *Nelumbo Nucifera*, this combined effect has been dubbed the "*Lotus-effect"* by Prof. Dr. W. Barthlott, a botanist from the University of Bonn, who discovered these characteristics[1].

This discovery of the Lotus-effect is of great technological interest. By transferring this effect to artificial surfaces, yielding surfaces that can be cleaned by a simple rainfall, numeral technical applications are possible. This essay focuses on the physical background of the Lotus-effect and several reported methods to synthesize such surfaces.

1. Physical basis of the Lotus-effect[2]

1.1 Foundations

Shown in figure 1 are the forces acting upon a liquid drop on a surface.

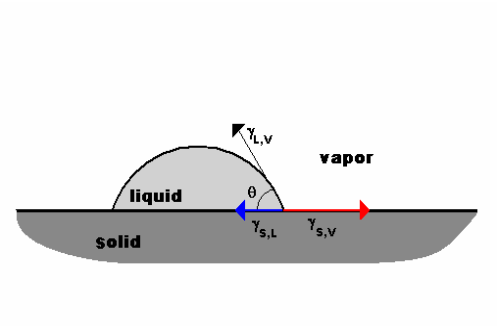

Figure 1: Forces acting on a liquid droplet on a solid.

Following simple goniometric rules, Young[3] derived that the contact angle θ_Y, from here onwards called Young's angle, is given by the relation [1]:

$$\cos\theta_Y = \frac{\gamma_{sv} - \gamma_{sl}}{\gamma_{lv}} \qquad [1]$$

, where γ_{ij} denotes the surface tension (energy per unit surface) of the interface ij and where s, l and v designate the solid, liquid and vapor phase. Equation [1] can also be derived from an energy consideration. The surface energy E can be given by equation [2]:

$$E = A_{lv}\gamma_{lv} + A_{sl}\gamma_{sl} + (A_s - A_{sl})\gamma_{sv} \qquad [2]$$

, in which A_{ij} is the surface area between the phases i and j, and A_s is the total surface of the solid. Minimizing E at constant volume as done by Blokhuis et al[27]. yields equation [1], independent of the shape of the drop.

Several remarks can be made about Young's equation:

1. Forces acting in the vertical direction are not taken into consideration. Since the surface tension exerts all along the liquid/vapor contact, there must also be an

opposing force acting on the solid, which the solid resist because of its elasticity. Roughly, Hooke's law indicates that deformation should be in the order γ_{lv}/E where E is the Young's modulus of the solid. For hard solids, this deformation is hardly observable. However, for soft solids like gels an obvious deformation can be seen.

2. Recent research by T. Pompe et al[4] has shown that for tiny drops, the contact line tension τ (excess free energy of a solid-liquid-vapor-system per unit length of the contact line) should be taken into consideration. A characteristic length scale for the influence of τ can be calculated by relating a typical value of τ to a typical value of γ, which yields $\tau/\gamma = 10^{-11}$ J m^{-1} / 10^{-2} J m^{-2} = 1 nm. Thus for droplets smaller than 1 μm, a measurable influence can be expected from the contact line tension and an angle correction should be made in the order of $\tau\kappa/\gamma$, where κ is the curvature of the contact line.
3. While surface tensions in a large range have been measured, varying between 20 mN/m to 1000 mN/m, there is no rule stating that the ration γ_{sv}-γ_{sl} / γ_{lv} has to be smaller than unity. Two cases seem to be of particular interest:
   (A) If γ_{sv}-γ_{sl} is larger than γ_{lv}, the drop tends to spread completely over the solid, resulting in a situation of complete wetting (θ = 0°)
   (B) If γ_{sv}-γ_{sl} is a lot smaller than γ_{lv}, the drop should be sitting on the solid like a marble (θ = 180°). However, no physical systems have been reported which realizes such a situation. For example, water on highly hydrophobic smooth surfaces make contact angles in the order 120°. One of the aims of this paper is to present methods on creating water-solid interactions in which the solid behaves as a superhydrophobic solid (θ > 150°).
4. Young's equation assumes the solid surfaces to be perfectly smooth and chemically homogenous.

1.2 More realistic surfaces

1.2.1 Rough surfaces[5]

Wetting in reality is more complex than described above. This is mainly due to the non-ideality of the surface, which can be both rough and chemically

heterogeneous. While the latter can be accounted for by considering a locally different compound with different properties (and thus a different surface tension), the former can't be corrected this easily. The earliest work on the effect of surface roughness on contact angles can be attributed to Wenzel[6] and Cassie and Baxter[7]. They provided different expressions for apparent contact angles, based on different average characteristics of a rough surface.

Wenzel assumed the liquid fills up the grooves in on a rough surface (figure 2a) and stated that on a rough surface for an identically same increase in the free liquid area at the upper surface of the drop (i.e. the liquid-vapor-surface), a greater amount of actual surface is wetted under it than compared to a smooth area. Thus, the net energy decrease on wetting a water-repelling surface will be greater for the rougher surface than a smooth surface and thereby enhances its water-repellency. The same analogy goes for water-attracting surfaces, thus making them more water attracting. Therefore, according to Wenzel, a distinction must be made between the total (or actual) surface and the superficial (or geometric) surface. This results in a "roughness factor" designated by r, the ratio between the actual surface and the geometric surface, by which the contact angle derived from Young's equation [1] must be corrected.

$$\cos\theta_W = r\cos\theta_Y \qquad [3]$$

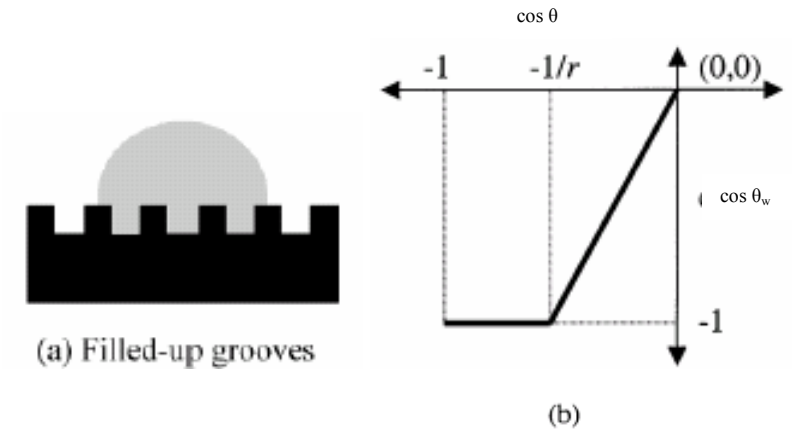

Figure 2. (a) Drop on a rough surface in Wenzel's model: the drop fills the grooves. (b) The apparent contact angle as predicted by Wenzel plotted against the angle according to Young's Law. (From Patankar[5])

In figure 2b is shown a plot of Young's contact angle against the apparent angle predict by equation [3]. Since r > 1, the Wenzel's angle is 180° when cos θ_Y < -1/r. Hence, according to Wenzel, the apparent angle is 180° for all cases in which θ_Y > $\cos^{-1}$ (-1/*r*). Experimental date provided by Onda et al.[8] showed agreement with Wenzel's theory.

In the approach of Cassie and Baxter it is assumed that the liquid forms a composite surface on the rough substrate (Figure 3a), i.e. the liquid does not fill the grooves on the rough surface. In this case, the liquid-surface interface is actually an interface consisting of two phases, namely a liquid-solid interface and a liquid-vapor interface. When a unit area of the surface has a surface fraction φ_1 with contact angle $\theta_{y,1}$ and an area fraction φ_2 with contact angle $\theta_{y,2}$, the apparent angle θ_C can be expressed by the following equation:

$$\cos\ \theta_C\ =\ \varphi_1\ \cos\ \theta_{Y,1}\ +\ \varphi_2\ \cos\ \theta_{Y,2} \qquad [4]$$

Applying this equation to a rough surface trapping air in the hollows of the surface, φ_2 then represents the area fraction of the trapped air. This modifies equation [4] to equation [5], with φ_S being the area fraction of the solid-liquid interface:

$$\cos\theta_C = \varphi_s \cos\theta_Y + (1-\varphi_S)\cos 180^{\circ} = \varphi_s \cos\theta_Y + \varphi_S - 1 \qquad [5]$$

Similar to figure 2b, the predicted contact angle using Cassie's equation [5] has been plotted against the angle according to Young's law in figure 3b.

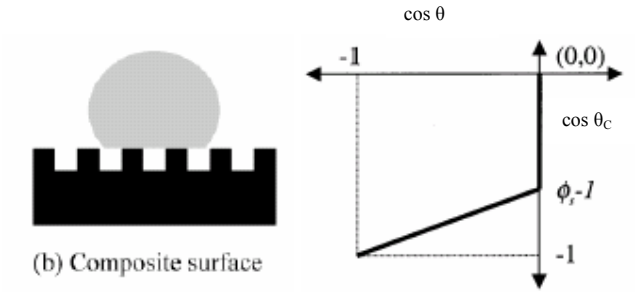

Figure 3. (a) Drop on a rough surface in Cassie's model: the drop sits on the spikes. (b) The apparent contact angle as predicted by Cassie plotted against Young's angle. (From Patankar[5])

The plot in figure 3b is quite different from the plot in figure 2b: according to Cassie's formula, the apparent contact angle changes sharply at $\theta_Y = 90°$ ($\cos \theta_Y = 0$). Furthermore, the apparent angle can only be 180° if Young's angle is 180°. Bico et al.[9] reported good agreement between Cassie's theory and their experiments.

1.2.2 Hysteresis of the contact angle

Another complexing factor is commonly called the hysteresis of the contact angle, i.e. different contact angles can coexist along the contact line. This can be observed rather easily: small drops of liquid can remain immobile on a tilted surface (like smaller rain drops on a vertical window). These droplets have a smaller angle at the back of the drop (at the receding end, with contact angle θ_r), and a larger angle on the front of the drop (at the advancing end, with contact angle θ_a), generating a capillary force to balance the weight of the drop[10].

This hysteresis, commonly denoted $\Delta\theta$, can be the result of different effects. Firstly, it can be the effect of chemically heterogeneity of the surface: consider a surface on which the contact angle is θ_1 on one end and θ_2 on the other end, the contact angle will vary between these two extremes on the contact line. The same reasoning applies to a discontinuity of the surface roughness, leading to different angles as described in section 1.2.1.

Measurements on the hysteresis of the contact angle have been done by Johnson and Dettre[11]. Data reported on the advancing contact angle θ_a and the receding contact angle θ_r on surfaces of wax with variable roughness is shown in figure 4.

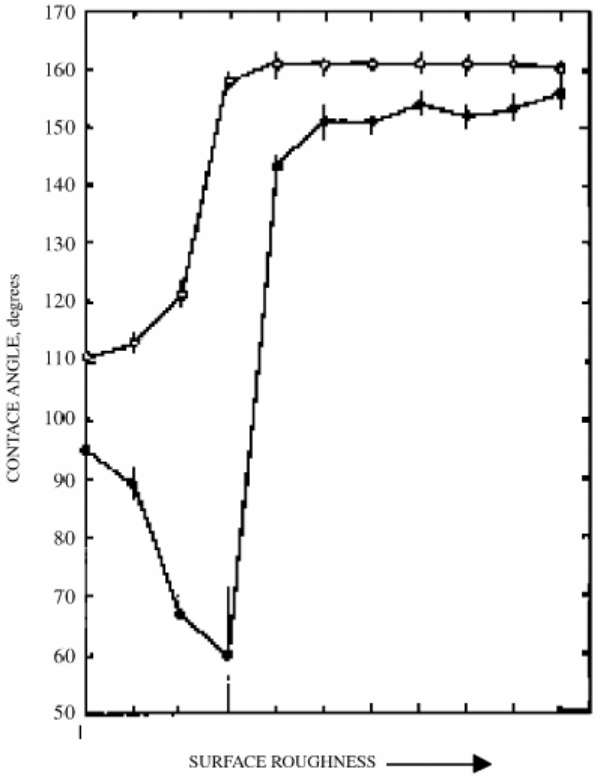

Figure 4: Advancing (open symbols) and receding (closed symbols) contact angles of water on a wax surface as a function of the surface roughness (From Johnson and Dettre[11])

Of interest is the effect of the surface roughness on the hysteresis. As the roughness (here defined only qualitively), increases, we first notice a large increase in hysteresis, although the variations of the angles themselves are relatively small. Then, as the roughness increases further, the hysteresis nearly vanishes due to the large increases in the contact angles. Thus, increasing surface roughness not only enhances the hydrophobicity of a hydrophobic surface, as predicted by the Wenzel-model and the Cassie-Baxter-model, but also has a large effect on the contact angle hysteresis.

1.3 Contact angle measurements

Different approaches can be used for measuring contact angles of non-porous solids, a goniometric approach and a tensiometric approach, with both having their advantages and their drawbacks. Another approach is used when measuring

the angles of porous substrates, involving the use of a tensiometer and the Washburn method. These three approaches shall be described briefly in the following sections.

1.3.1. Goniometry[12]

The basis for the goniometric approach is the analysis of the shape of the drop. The contact angle can be found directly by measuring the angle formed between the solid and the tangent of the drop of an image made of the drop. A typical goniometric instrument consists of a light source, sample stage, lens and image capture. Hysteresis can also be measured using the goniometric approach: the advancing contact angle is measured by slowly adding liquid to the drop, while the receding contact angle can be measured by slowly removing liquid from the drop, either by evaporation of by removal of the liquid directly.

The large advantage of goniometry comes from its relative simplicity. It can used for almost any solid, as long as it has a relatively flat portion or a regular curvature and can be fitted on the stage of the instrument.

The main disadvantage of the goniometric approach is the subjectivity of the researcher in assigning the tangent line. This problem can be reduced by computer analysis of the droplet shape. The requirement of a surface large enough a hold a droplet is another problem, yielding the goniometric approach a very poor technique for measurements on fibers.

1.3.2. Tensiometry[13]

The tensiometric method measures the forces that are present when a sample of solid is brought into contact with a test liquid. The contact angle can than be calculated when the forces of interaction, the surface tension and the geometry of the solid is known. Firstly, the surface tension of the liquid is measured, usually with either a Wilhelmy plate or a DuNouy ring. Then, a sample of the solid to be tested is hung to a balance above the liquid. When the liquid is raised it comes in contact with the solid and a different force is detected on the balance. The point at which the solid contacts the liquid is called the zero depth of immersion. If the solid is put deeper into

the liquid, the detected force is a sum of the wetting force, the weight of the probe and the buoyancy. The weight of the probe can be measured beforehand and set to zero, while the effect of the buoyancy can be removed by extrapolating the force back to the zero depth of immersion, leaving the resulting wetting force. This wetting force is defined as the product of the surface tension between the liquid and the vapor, the perimeter of the probe and the cosine of the contact angle. The contact angle obtained from this calculation is the advancing contact angle θ_a when the solid is immersed in the liquid, and the receding contact angle θ_r when the solid is retracted from the liquid. Static contact angles can be estimated by reducing the rate of immersion or retraction.

There are many advantages of the tensiometric approach over the conventional goniometric method. Hysteresis can be easily measured easily. Contact angles on fibers, which posed a problem for the goniometric approach, can be measured with the tensiometric approach. Coatings can also be measured by coating a simple solid substrate before measuring. One final advantage is the measurement is down around the entire perimeter of the immersed solid, giving an averaged value for the contact angle.

Tensiometric measurements also have two large constraints. Firstly, the enough liquid must be available to immerse the solid in. Secondly, there are several requirements for the solid sample. It must be formed in such geometry so it has a constant perimeter over a portion of its length. It must also have the same surface on each side that contacts the liquid and be small enough to be hung to the balance of the tensiometer.

1.3.3. Washburn method[14]

The wetting of powder and porous structures is difficult to measure due to the complication of trapping liquid in this the pores. A method for solving this has been developed by Washburn: if a porous solid is put into contact with a liquid, liquid will rise in the pores according to the following relationship:

$$T = \left(\frac{\eta}{C\rho^2 \gamma \cos\theta} \right) M^2 \qquad [4]$$

, in which T denotes the time after contact, M the absorbed mass, θ the contact angle, C a material constant and η, ρ, γ the viscosity, density and surface tension of the liquid respectively. A graph of the absorbed mass squared versus time yields a straight line with slope η / C ρ^2 γ cos θ. The viscosity, density and surface tension can be measured from other experiments, leaving two unknowns, the material constant C and the contact angle θ. Washburn experiments determine C by the use of a test liquid with low surface tension, resulting into complete wetting. Thus, setting θ to zero, the material constant C can be calculated and the solid can be used against various liquids.

1.4 The Lotus-effect

In order to describe the background of the Lotus-effect, an exact definition is in order: a surface which shows the Lotus-effect is superhydrophobic, expressed by a contact angle larger than 150°. Due to this superhydrophobicity, water tends to roll off the surface, even if the surface is tilted slightly, and cleans the surface of a contamination in its way (Figure 5).

Figure 5: A droplet takes up the dust covering a lotus leaf. (From http://www.botanik.uni-bonn.de/system/lotus/en/prinzip_html.html).

How does a lotus leaf acquire this superhydrophobicity? Starting from the late 1970's, scanning electron microscopic studies on biological surfaces have revealed a large micro structural diversity. A lot of plants showed a combination of microstructure and nanostructure on their surface which minimizes the contact area

with anything that came into contact with the surface. The leaves of a lotus plant showed epidermal cells on its rough surface covered with wax crystals (figure 6).

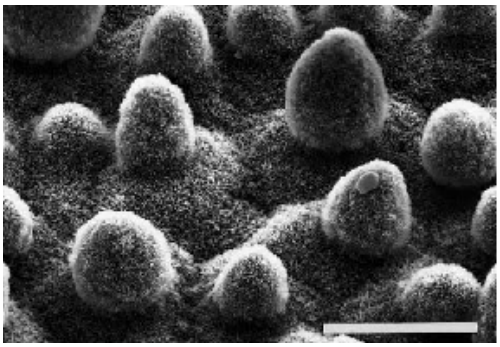

Figure 6: SEM-image of lotus leaf. The micro structural epidermal cells are covered with nanoscopic wax crystals. Bar: 20 µm. (From Barthlott et all.[1]).

Figure 7: A water droplet on a lotus leaf. (From http://www.botanik.uni-bonn.de/system/lotus/en/prinzip_html.html).

The wax crystals provide a water-repellent layer, which is enhanced by the surface roughness according to the models of Wenzel and Cassie. The wax crystals are badly wettable. As a result of this, water droplets on the surface tend to minimize the contact between the surface and the drop, forming a spherical droplet (figure 7). Contaminations on the surface are usually larger than the cellular structure of the leaves, leaving the particle resting on the tips of the latter. As the result, the contact area and thus the interfacial interaction is minimized (figure 8a). When a water droplet rolls over the contamination, energy through absorption is gained, even is the particle is hydrophobic. The particle is then removed from the surface if the energy gained by absorption to the water droplet is larger than the energy it costs to remove the particle from the leaves, which is usually the case due to the small contact area (figure 8b/c).

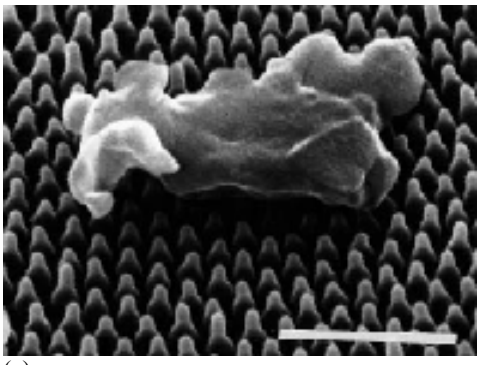

(a)

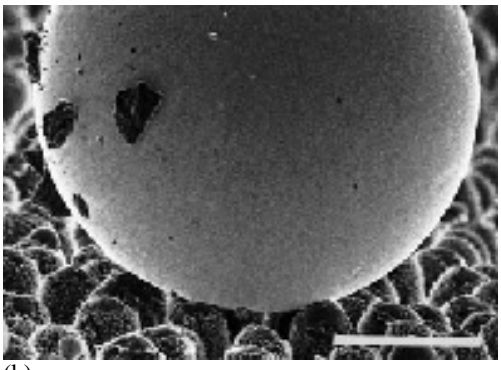

(b)

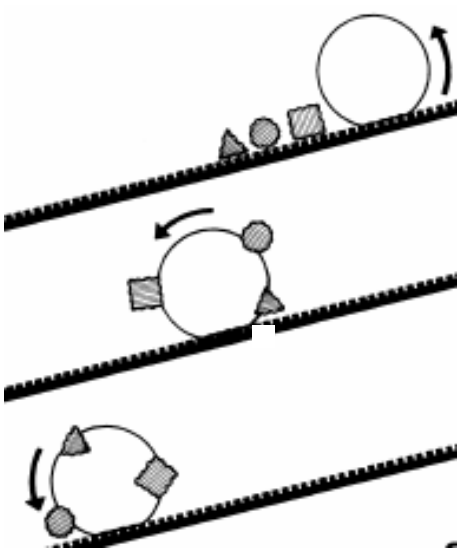

(c)

Figure 8: (a) Contaminating particle on a regularly sculptured wing surface of *Cicada orni* (a plant with a surface structure similar of that of a lotus plant), demonstrating the decreased contact area between a particle and a rough surface. Bar*:*1 µm (b)The Lotus-effect: contaminating particles adhere to the droplet and are removed when the droplet rolls off the surface. Bar: 50 µm. (c) Diagram showing the cleaning process of a rought surface. (From: Barthlett[1]).

2. Wenzel's and Cassie's model: which applies in what situation?

Several researches have been done after the effects of surface roughness on the interaction between a solid and water. Onda et al[8]. claimed agreement with Wenzel's model, whereas research by Bico et al[9]. verified Cassie's model. It was not conclusive which model applies in a given situation, until a recent article by Patankar[6]. These three articles shall be discussed briefly.

2.1 Onda et al.: Contact angles on a fractal surface[8]

In this research, Onda et al. studied the contact angles of with use of water and aqueous solutions of 1,4-dioxane in various concentrations on a flat alkylketene dimer (AKD) surface and a fractal AKD surface (figure 9) and compared it with Wenzel's equation with some small modifications.

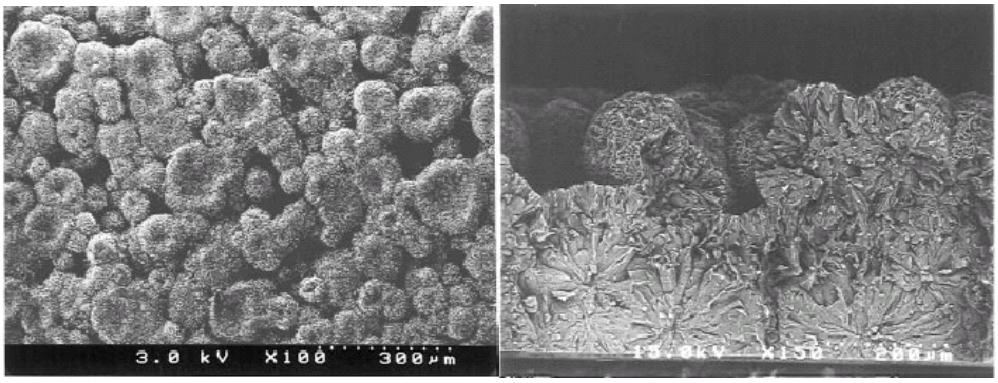

(a) (b)

Figure 9: SEM-images of a fractal AKD surface: (a) top view (b) cross section (From Onda et al.[8])

Measurements have been made as follows: drops of liquid were brought onto the surface, after which the surface is vibrated vigorously to acquire an equilibrium state. A droplet of water on the fractal AKD surface showed a contact angle of 174˚, which can truly be called superhydrophobic, whereas a water drop only forms contact angles of 109˚ on a flat AKD surface, showing that the surface roughness indeed enhances the hydrophobicity of the surface. Measurements with various aqueous 1,4-dioxane solutions have also been made. The results are summarized in figure 10.

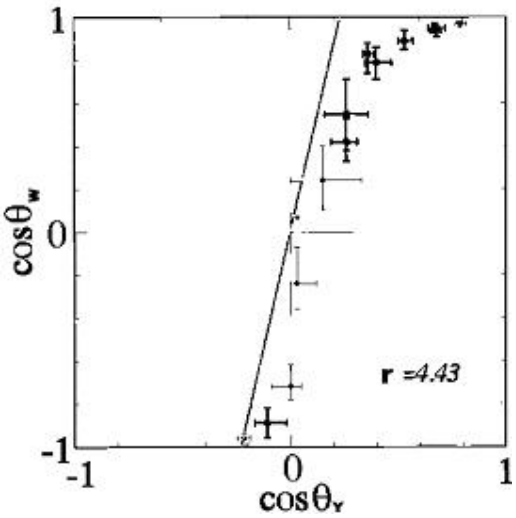

Figure 10: Plot of measured angles on the fractal surface ($\cos \theta_W$) compared with measured angles on the flat surface ($\cos \theta_Y$). The solid line represents the predicted relationship.

As can be seen in figure 10, the results obtained from this experiment show good agreement with Wenzel's model.

2.2 Bico et al.: Effects of some surface structures: stripes, cavities and spikes[9]

Bico et al. investigated the effect the effect of some surface structures on their hydrophobicity, namely a spikes structure, a cavities structure and a stripes structure. SEM-images of these structures are shown in figure 11.

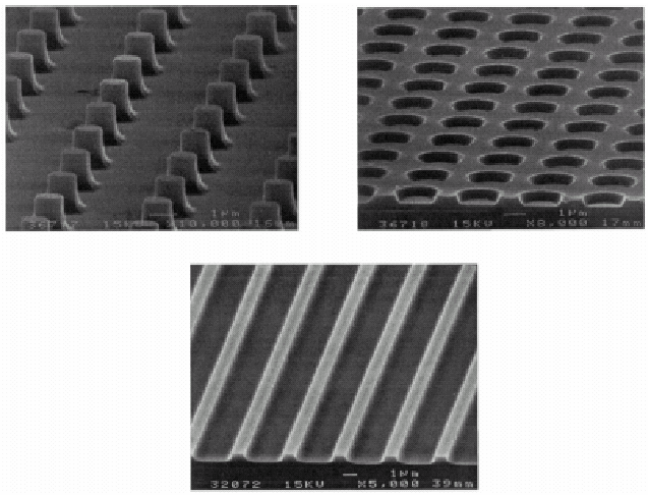

Figure 11: SEM-images of the surface structures designed for the research of the effect of the pattern on the contact angles. (From Bico et all[9])

The contact angles of water on these surfaces were measured and compared with theoretical contact angles calculated using Cassie's equation (equation [5]). The results are shown in table 1.

Pattern	φ_s	θ_a	θ_r	θ_c
Plane	1	118	110	
Holes	0.64	138	75	131
Stripes (orthogonal)	0.25	165	132	151
Stripes (parallel)	0.25	143	125	151
Spikes	0.05	170	155	167

Table 1: Measurements of the solid fraction φ_s, the advancing and receding contact angles. These contact angles are compared with the contact angles given by Cassie's equation.

For the cavities structure and the spikes structure the found advancing contact angles are in close agreement with the angles predicted using Cassie's law. The large contact angle found for the spikes structure indicates the drop is indeed nearly spherical. The superhydrophobicity of the spikes structure is confirmed by the large value of the receding contact angle: this surface really behaves highly water-repellent. The cavities structure cannot be considered superhydrophobic. This can be ascribed to the large area fraction of the solid, which, by Cassie's equation, makes the contact angle smaller. A large hysteresis can also be seen between the receding

and advancing contact angle. Bico et al. ascribes this to shallowness of the cavities, which retain water at the retraction, which can be confirmed using Cassie's equation (equation [4]), considering a solid-water interface on the area fraction φ_s and a water-water interface (contact angle 0˚) over the area fraction 1-φ_s.

The effect of the stripes can be measured in two directions, one parallel to the stripes and one orthogonal to the stripes. As can be seen in table 1, both the contact angles and the hysteresis are largely influenced by the direction of wetting.

The main conclusion that can be drawn from this research is that the contact angle mainly depends on the area fraction of the solid (φ_s) rather than the surface roughness and thus shows that in the given circumstances the contact angles abide Cassie's equation rather than Wenzel's equation.

2.3 Patankar: On the modeling of contact angles on rough surfaces[5].

As shown in the previous researches it is not conclusive whether Wenzel's model or Cassie's model applies for a certain situation. Moreover, as reported by Bico et al.[9], a drop following Cassie's model can be induced to follow Wenzel's model. Patankar recognized this problem and stated two criteria for a robust superhydrophobic surface: the apparent contact angle should not change when a transition occurs between Wenzel's angle and Cassie's angle and this apparent angle should be as close to 180˚ as possible.

From an energy analysis, Patankar derived both situations are local equilibrium states. Since energy has to be applied to incur transitions between the states, it can be concluded some energy barrier exist between this two states.

Patankar also analyzed which of these two local energy minima corresponds with a global minimum. Using the same energy analysis, Patankar derived for the energy of a drop on a surface in equilibrium:

$$\frac{G}{\sqrt[3]{9\pi}V^{2/3}\sigma_{lv}} = (1-\cos\theta_O)^{2/3}(2+\cos\theta_O)^{1/3} \qquad [6]$$

In this equation G denotes the Gibbs free energy, V the volume of the drop and θ_O the observed contact angle (which can be either Wenzel's contact angle or Cassie's contact angle). The left-hand side of the equation denotes nondimensional energy. It is clear that the right hand side is a monotonously increasing function of θ_O. As a result, a drop shape with a lower observed contact angle has a higher energy (i.e. if $\theta_C < \theta_W$, a drop following wetting the entire rough surface will be of lower energy than a drop sitting on the spikes). The values of θ_C and θ_W are again given as a function of θ_Y in figure 12.

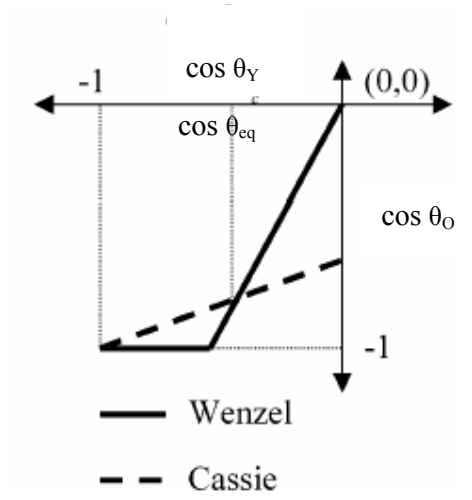

Figure 12: Prediction of the observed contact angle θ_O by Wenzel and Cassie as a function of Young's angle. For $\theta_Y = \theta_{eq}$, the contact angle predicted by Wenzel has the same value's the contact angle predicted by Cassie. (From Patankar[5])

It is apparent from figure 12 that for $\theta_Y = \theta_{eq}$, we have $\theta_W = \theta_C$. Since according to equation [6] a lower value of θ_O corresponds with a lower energy, it can be concluded that for liquids with $\theta_Y > \theta_{eq}$, the Wenzel's situation has a lower energy than Cassie's. The opposite goes for $\theta_Y < \theta_{eq}$.

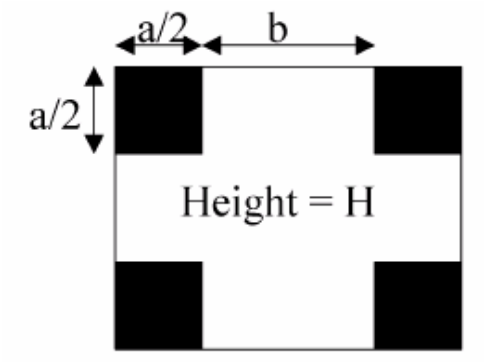

Figure 13: Top view of one period of roughness geometry proposed by Patankar. Of each of the pillars one quarter is shown. (From Patankar[5])

Thus, in order to design a robust superhydrophobic surface, one has to take the energy analysis above in consideration. In the same article, Patankar proposes a design procedure: considering geometry of square pillars of size *a* x *a*, height *H*, and spacing *b* arranged in a regular array (Figure 13) with a given Young's angle. Then the values of a, b and H should be arranged in such a way that $\theta_W = \theta_C$. Evaluating equation [3] and relation [5] for the given situation gives relations [7] and [8], which are plotted in figure 14.

$$\cos\theta_C = \frac{(1+\cos\theta_Y)-1}{\left(b/a+1\right)^2} \qquad [7]$$

$$\cos\theta_W = \left(1+\frac{4}{\left(b/a+1\right)^2\left(a/H\right)}\right)\cos\theta_Y \qquad [8]$$

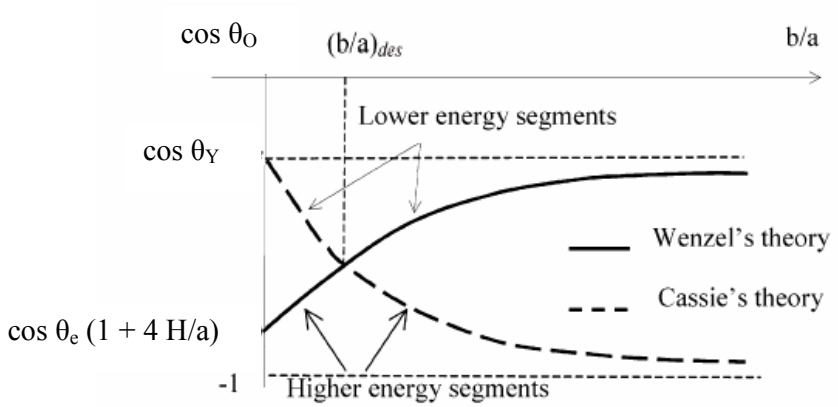

Figure 14: Plot of the apparent contact angles predicted by Wenzel and by Cassie for the geometric situation given in the text. (From: Patankar [5])

As can be seen in figure 14, only Wenzel's contact angle is dependent on the value of a/H. The curve is translated downward for a lower a/H ratio, thus bringing the intersection point closer to –1. Also, it is shown that the intersection point has the largest contact angle of all the possible lower energy states. Thus, the design the robust surface as defined before ($\theta_C = \theta_W$ and close to 180˚), it is needed to use the intersection point as a design condition and make the ratio a/H very small, e.g. a forest of tall, slender nanopillars with appropriate spacing. The same calculations can be done for different geometrical constellations.

In conclusion, Patankar showed from an energy analysis that both the contact angles predicted by Wenzel and predicted by Cassie are local energy minima. Furthermore, he derived that the smaller of Wenzel's and Cassie's contact angle is the one is the angle corresponding to the global energy minimum.

3. Synthesis of superhydrophobic surfaces

In the last years of the 1990's, a lot of reports have been made on the synthesis of superhydrophobic surfaces. Most of these methods involved the mechanical roughening of a hydrophobic surface such as machining and (plasma) etching[8-9,15-21]. However, other methods are also reported. Three of these shall be described below.

3.1 Transparent Superhydrophobic Thin Films with Self-Cleaning Properties

The hydrophobicity of most articificially created superhydrophobic surfaces gradually degrades during a long outdoor exposure due to the build up of stain, which natural superhydrophobic surfaces (water-repellent leaves) avoid by their wax metabolism. However, such a metabolism is hard to duplicate on a man-made surface. Nakajami et al.[22] recognized this problem and developed a procedure to create transparent superhydrophobic films with a enhanced self-cleaning property.

The synthetic procedure in short is as follows: A boehmite (AlOOH) powder, acetylacetonate (AACA) and various concentrations of titanium acetylacetonate ($TiO(C_5H_7O_2)_2$, TACA) were mixed with ethanol. In order to dissolve the AACA, the mixture was sonicated. The resulting mixtures were coated on Pyrex glass plates. After drying, the plates were calcinated to evaporate the AACA, leaving a surface roughness. These plates were then immersed in a methanol solution of hydrolyzed (heptadecafluorodecyl) trimethoxysilane ($CF_3(CF_2)_7(CH_2)_2Si(OCH_3)_3$, FAS-17), which served as the water-repellent agent.

This procedure resulted in glass plated coated with both a water repelling film and a boehmite film containing 0 – 71 wt% TiO_2. The TiO_2 is formed by a thermal decomposition of TACA and serves as a strong oxidation photocatalyst in UV-illumination[23], able to oxidize most organic stains in to carbon dioxide[24].

After synthesis, the glass plates were tested on three criteria: transparency, superhydrophobicity and durability. The contact angle on the synthesized films

varied from 148.1˚±1.70˚ (0 wt% TiO_2) to 155.6˚±1.0˚ (71 wt% TiO_2) and thus can be considered superhydrophobic. Increasing the weight percentage of the TiO_2 resulted in a small increase on contact angle, which is mainly caused by the increasing surface roughness (Fig 15).

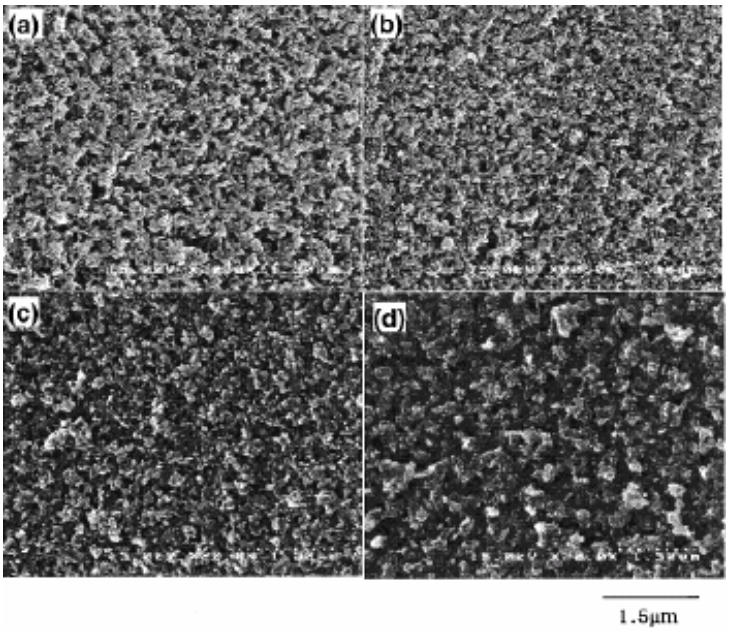

Figure 15: SEM images of boehmite – TiO_2 films: (a) 0% TiO_2 (b) 20% TiO_2 (c) 55.6% TiO_2 (d) 71.4 % TiO_2. (From: Nakajami et al.[22])

Transparency seems theoretically to be competitive with the superhydrophobicity, since a surface with increasing roughness also becomes more a source for light scattering. Transmittance measuring of the prepared films confirmed this theory (fig 16). For films up to 20 wt % TiO_2, the transmittance is almost 100%. Above 20 wt %, transmittance is reduced noticeable. This confirms surface roughness increases with TiO_2-concentrations, which can attributed to the amount of large TACA-molecules before it decomposes into TiO_2 during calcinations.

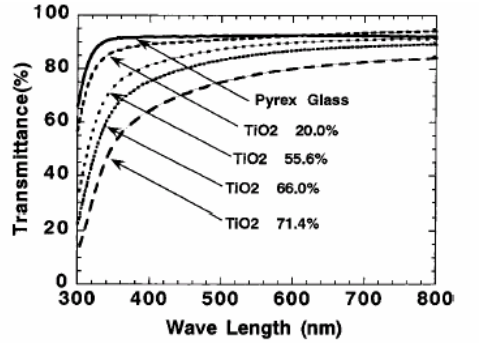

Figure 16: Transmittance of light in the visible wavelength range for the prepared films. (From: Nakajami et al.[22])

The third criterion, durability, was also tested with several methods. Illumination with UV-light showed a decrease in contact angle that became larger with illumination time and TiO_2 concentration (figure 17), which can be accounted for by the decomposition of FAS-17 in a photocatalytic reaction. With small concentrations however, the contact angle decreased only slowly. A similar result was found for measurements of the contact angle after outdoor exposure (fig 18). What should be noted with this is the smaller decrease in contact angle for a film with a small concentration of TiO_2 than a film without TiO_2. While the build up of stain on the surface can easily explain this, it is less trivial why a higher amount of TiO_2 leads to a faster decay of the superhydrophobic surface. One of the possible explanations for this result is the difference of kinetic balance of the decomposition between stain and FAS-17. This balance depends on the concentration of TiO_2 and particle sizes of the starting materials. Thus, it will be important to obtain the optimum balance by controlling these key factors for the proper performance of the films.

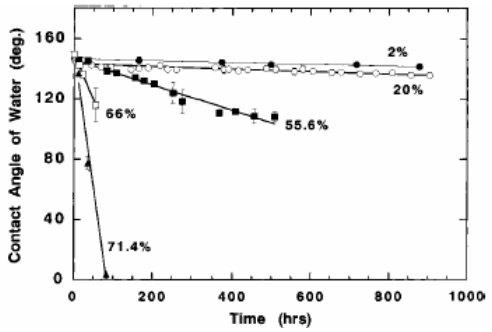

Figure 17: Change of contact angles as a result of UV-illumination. (From: Nakajami et al.[22])

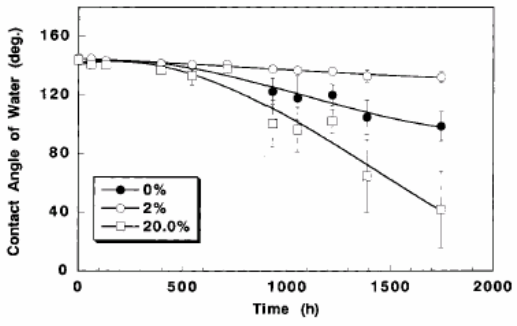

Figure 18: Change of contact angles as a result of outdoor-exposure. (From: Nakajami et al.[22])

One of the possible explanations for the enhanced self-cleaning is the production of radicals by UV-illumination of TiO_2. These radicals then diffuse through the FAS-17 layer to decompose the stains.

Thus, Nakajami et al. developed a procedure to produce films transparent durable superhydrophobic films. This procedure has a couple large advantages. It has a large degree of transparency and can be tuned to maintain it's superhydrophobicity for a long time, which shows promising results in prospect of industrial manufacturing of superhydrophobic surfaces for every day use. The main disadvantage is the tedious procedure.

3.2 Transformation of a simple plastic into a superhydrophobic surface

Recently, Erbil et al.[25] reported a simple and inexpensive method to form a superhydrophobic coating using polypropylene, which can be applied to a large variety of surfaces.

Polypropylene was slowly dissolved in a fixed volume of p-xylene at 130 °C. This polymer solution was then put onto glass slides. The coating was established by evaporating the solvent in a vacuum oven or by addition of a non-solvent (precipitator).

The effects of the polymer concentration and the film formation temperature on the homogeneity, surface roughness and water contact angle have been investigated. Raising the concentration of the polymer solution increased both the coating thickness and the surface roughness, raising the contact angle from 104° for a smooth polypropylene surface to 149° for a coating obtained with a 40 mg/ml solution. However, the coating was inhomogeneous with cracks throughout the entire coatings. Varying the drying temperature also had an influence on the inhomogeinity. At lower drying temperature, the solvent evaporation rate is slower and the nucleation time is increased, leading to a higher crystallinity. However, a lower drying temperature also increased the nucleation rate, resulting in a loose network. Overall,

lower drying temperature yielded a more inhomogeneous coating with a higher surface roughness and higher contact angles (fig. 19)

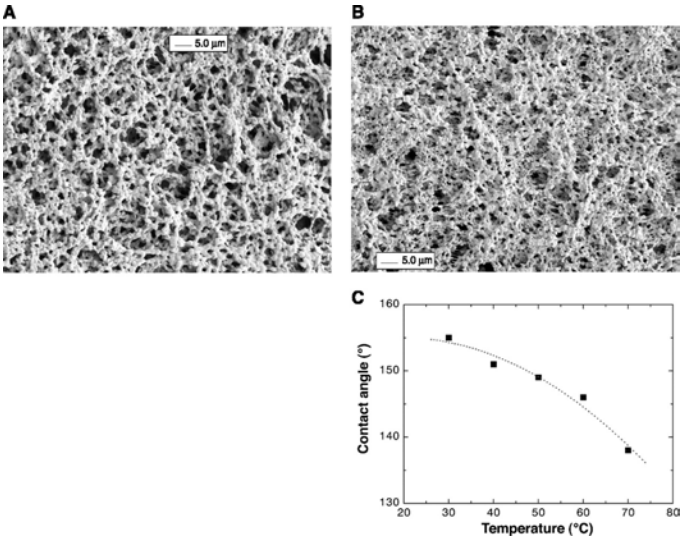

Figure 19: SEM images of polypropylene coatings obtained from a solution (20 mg/ml) in p-xylene on glass slides. The drying temperatures were (**A**) 30°C and (**B**) 60°C., at which the solvent was evaporated using a vacuum oven. The surfaces were sputter-coated with 1-nm-thick gold before the measurements were taken. The measurements were taken at 1 KeV. The magnification is ×1000. (**C**) The variation of water contact angle with the drying temperature on the superhydrophobic i-PP coating obtained from a solution (20 mg/ml) in p-xylene on glass slides. (From: Erbil et al.[25])

As nonsolvents MEK, cyclohexanone and isopropyl alcohol were investigated. Of these three, MEK yielded the best homogeneity and the largest contact angle (160°). The effect of the use of a nonsolvent is the result of three impacts: first, they act as a polymer precipitator by increasing the polymer phase sepration, resulting in a smaller crystallization time. Also, since most nonsolvents are more volatile than the p-xylene, it increases the rate of evaporation and decreases the time needed for crystal formation. Then, addition of nonsolvents containing oxygen increases the wettability of the polymer solution on the glass resulting from the presence of OH-groups on the glass surface. This gives a more homogenous initial layer over which a more homogenous coating grows.

The durability of the coatings was also tested in terms of adhesion, compressive forces, ambient temperature, nano-scratch resistance and

contamination. Most of the test showed the coating was rather durable under normal circumstances for at least a couple of months.

In summary, this procedure is a relative simple procedure using inexpensive materials to create a superhydrophobic surface. Another large advantage the authors show is that almost every material can be coated this way (these coatings have also been prepared on aluminum foil, stainless steel, Teflon, high-density polyethylene, and polypropylene), as long as the solvent does not dissolve the surface material. A disadvantage could be the decay of durability on a longer term, as well as the question whether the material is transparent.

3.3 Non-stick water

All of the experiments referred to earlier in this paper have been on the modification of the solid surface to induce superhydrophobicity. Aussillous and Quéré[26] ingeniously inverted this idea and modified the liquid instead, by coating drops of water with a very hydrophobic powder (lycopodium grains of typical size 20mm covered with fluorinated silanes). This resulted in quasi-spherical droplets, with the only deformation being a result of the gravity. It behaves perfectly non-wetting on a glass plate (fig 20) and is shown even to float as a perfect “marble” on a pool of water.

Figure 20: A liquid marble: water coated with silane-treated lycopodium grains of typical size 20mm). (From: Aussillous[26])

Although the marbles produced this way doesn't directly lead to advancement in the creation of superhydrophobic surfaces, it does give insight in the fluid mechanical behavior of water droplets on superhydrophobic surfaces. The results of this experiment shall not be discussed in this paper.

4. Conclusion

The contact angle of a drop of liquid on a smooth solid surface is a relationship between the surface tensions of the three interface surfaces. The equation for calculation of this contact angle has been reported by Young in the 19th century. Modifications of Young's equation to take surface roughness into account have been proposed by Wenzel and Cassie & Baxter. Wenzel's model assumes the liquid wets the grooves on a rough surface, thus leading to a higher actual surface. Cassie and Baxter proposed the liquid sitting on the grooves and having gas trapped beneath it. Both models showed that the intrinsic liquid-affinity of the solid is enhanced by surface roughness, i.e. the hydrophobicity of hydrophobic surfaces is enhanced by surface roughness, as is the hydrophilicity of hydrophilic surfaces in the case of water, but predict different contact angles, which are both local energy minima.

The application of these models was found in nature with the lotus plant. On the leaves, a microstructure was found, enhancing the roughness of the leaves, leading to the self-cleaning property of this plant. This self-cleaning has been researched thoroughly and different methods have been reported to synthesize artificial surfaces with this self-cleaning property.

5. References

1. Barthlott, W.; Neinhuis, C. *Planta* **1997**, *202*, 1-8.
2. Quéré, David, **Rough ideas on wetting**, *Physica A* **2002**, *313*, 32-46.
3. Young, T. *Philosophical Transactions of the Royal Society of London* **1805**, *95*, 65.
4. Pompe, T.; Herminghaus, S. *Physical Review Letters* **2000**, *85,* 1930-1933.
5. Patankar, N.A. *Langmuir* **2003,** *19,* 1249-1253
6. Wenzel, R.N. *Industrial and Engeneering Chemistry*, **1936**, *28*, 988-994.
7. Cassie, A.B.D.; Baxter, S. *Transactions of the Faraday Society*, **1944**, *40*, 546-551
8. Onda, T.; Shibuichi, N.; Satoh, N.; Tsuji, K. *Langmuir* **1996**, *12* (9), 2125-2127.
9. Bico, J.; Marzolin, C.; Quere, D. *Europhys. Lett.* **1999**, *47* (2), 220-226.
10. Dussan, E.B.; Chow, R.T.P. *Journal of FluidMechanics* **1983**, *137*, 1 –29.
11. Johnson, R.E.; Dettre, R.H. *Advancments in Chemistry Series* **1964**, *43*,12 – 135.
12. KSV Instruments USA: http://www.ksvinc.com/contact_angle.htm,
13. KSV Instruments USA: http://www.ksvinc.com/wilhelmy_plate.htm
14. KSV Instruments USA: http://www.ksvinc.com/powder_wetting.htm
15. Coulson, S.R.; Woodward, I.; Badyal, J.P.S.; Brewer, S.A.; Willis, C. *Journal of Physical Chemistry B* **2000**, *104*, 8836.
16. Chen, W.; Fadeev, A.Y.; Hsieh, M.C.; Öner, D.; Youngblood, J.; McCarthy, T.J. *Langmuir* **1999**, *15*, 3395-3399.
17. Veeramasuneni, S.; Drelich, J.; Miller, J.D.; Yamauchi, G. *Progress in Organic Coating* **1997**, *31*, 265-270.
18. Nishino, T.; Meguro, M.; Nakamae, K.; Matsushita, M.; Ueda, Y. *Langmuir* **1999**, *15*, 432-4323.
19. Shibuichi, S.; Onda, T.; Satoh, N.; Tsujii, K. *Journal of Physical Chemistry B* **1996**, *100*, 19512-19517.
20. Öner, D.; McCarthy, T.J. *Langmuir* **2000**, *16*, 7777-7782.
21. Hozumi, A.; Takai, O. *Thin Solid Films* **1998**, *334*, 54-59.

22. Nakajami, A.; Hashimoto, K.; Watanabe, T.; Takai, K.; Yamouchi, G.; Fujishima, A. *Langmuir* **2000**, *16*, 7044-7047.
23. Kawai, T.; Sakata, T. *Nature* **1980**, *286*, 474.
24. Schwitzgebel, J.; Ekerdt, J. G.; Gericher, H.; Heller, A. *Journal of Physical Chemistry* **1995**, *99*, 5633.
25. Erbil, H.Y.; Demirel, A.L.; Avci, Y.; Mert, O. *Science* **2003**, *299* (5611), 1377-1380.
26. Aussillous, P.; Quéré, D. *Nature* **2001**, *411*, 924-927.
27. Blokhuis, E.M.; Shilkrot, Y.; Widom, B. *Molecular Physics* **1995**, *86*, 891-899.